Characteristic Linear Dynamics of Kinetically Controlled Burning

Part I: Traditional Single-Reactor Models

C. Martin[1], J. Ranalli, U. Vandsburger, W. Baumann

Virginia Active Combustion Control Group
Virginia Polytechnic Institute & State University, Blacksburg

[1]Corresponding Author: chmarti1@vt.edu

We examine combustion controlled predominantly by chemical kinetics using various incarnations of the Well Stirred Reactor. The model is presented in canonical forms exhibiting first- and higher-order responses to both flow rate and mixing perturbations. These behaviors are completely characterized by physically relevant dimensionless quantities. Furthermore, because of their relevance to thermo-acoustic instabilities, we generate quasi-minimal degree-of-freedom formulations relating inlet conditions and heat release rate for both single-step and generalized multi-step chemical kinetic models.

Keywords: WSR, CSTR, linearized, dynamic, heat release rate

Nomenclature

β ..... Thermal eccentricity
Γ .... NSH WSR reaction sensitivity
$\nu'_{i,j}$ ..... Reactant rxn. coef.
$\nu''_{i,j}$ ..... Product rxn. coef.
ϕ ..... Species rxn progress
ψ ..... Thermal rxn progress
ρ ..... Density
τ_c ..... Chemical time
τ_r ..... Residence time
ζ_i ..... Reaction rate spec. i

$\mathbf{A}$ ..... State matrix
$\mathbf{B}$ ..... State input matrix
$\mathbf{C}$ ..... State output matrix
$\hat{c}$ ..... Specific heat eccentricity
c_p ..... Specific heat
$c_{p,r}$ ..... Specific heat of reactants
$c_{p,p}$ ..... Specific heat of products
$c_{p,i}$ ..... Specific heat of species, i
Da ..... Damköhler number
h ..... Enthalpy
h_p ..... Enthalpy of products
h_r ..... Enthalpy of reactants
h_i ..... Enthalpy of spec. i
Δh ..... Enthalpy of reaction
$\dot{m}$ ..... Mass flow
MW_i ... Molecular weight of spec. i
$\mathbf{P}$ ..... Transformation matrix
q_j or $\mathbf{q}$ ..... Reaction rate vector
Q ..... Heat release rate
R ..... Normalized reaction rate
$\hat{R}$ ..... Dimensionless reaction rate
s ..... Laplace variable
T ..... Reactor temperature
T_a ..... Activation temperature
T_{inlet} ..... Inlet temperature
ΔT ..... Adiabatic change in T
u ..... Mass flow excitation
$\mathbf{U}$ ..... State input vector
v ..... Equivalence ratio excitation
V ..... Reactor Volume
$V_{i,j}$ or $\mathbf{V}$ ..... Rxn. coef. tensor
$\mathbf{X}$ ..... Linear state vector
Y_i or $\mathbf{Y}$ ..... Mass fraction vector
$Y_{i,inlet}$ ..... Inlet mass fractions
ΔY_i ..... Adiabatic change in Y_i
$\mathbf{Z}$ ..... Transformed state vector

1. Introduction

A wide variety of incarnations of the Well Stirred Reactor (WSR) exist to describe the dynamics of chemical kinetics in a homogeneous reaction region. Though these are as varied in formulation and in solution as the reactions they describe, there are common behaviors that bind them and that imply simpler, canonical formulations might be possible. In the case of kinetically controlled combustion, the WSR is singularly appropriate, since its very formulation places focus on the chemical kinetics while minimizing all transport phenomena save convection. Furthermore, it is typically heat release rate that is of primary importance to a combustor, so it is with that in mind that we study the dynamics that separate velocity and mixing perturbations and the heat release rate of a homogeneous reaction region using the WSR.

The WSR's derivation is predicated on the assumption that all transport phenomena in the reactor are significantly faster than the chemical reaction rate. While the ability to ignore spatial gradients and model reacting flows with ODEs instead of PDEs makes the WSR quite attractive transport times only out-pace chemical times when the turbulent Damköhler number is less than unity[1, 16].

As we shall reiterate here, one must be very cautious when using WSRs to capture dynamic heat release since they are very poor predictors of the behaviors in most practical combustion systems. For systems in which WSRs are appropriate, however, there are a number of common simplifying assumptions whose impact on the flame dynamics can be parametrically quantified. Here, we derive canonical forms for the WSR subject to velocity and mixing perturbations and show the linear dynamic characteristics for three of the most common realizations for the WSR:

1. The *Simple WSR*

constant c_p, single step reaction rate, constant volume,

2. The *Non-Simple Enthalpy WSR*
   c_p is variable across species and temperature, single step reaction rate, constant volume,

3. The *Mutli-Step Chemical Kinetic WSR*
   constant c_p, n-step chemical kinetics.

In each case, we quantify the impact of the various thermal and chemical kinetic properties that are introduced to the system with dimensionless parameters where possible.

1.1 Background

The WSR has been the object of countless investigations into the dynamics of chemically reacting flows.

Good progress has been made with the WSR in the field of thermo-acoustic instabilities in gas turbines. Since pressure oscillations in these systems have proven to be a small percentage of the mean[4], the WSR has no dependency on the momentum equation and the dynamics are somewhat simpler than in works when pressure oscillations are important. Liewen et. al. studied the effect of flow rate oscillations[5] as well as mixture oscillations[5]. Park et. al. applied linearized WSRs in a system-level model with simple single-resonance acoustics to predict instabilities[15]. Martin used DC gains predicted by the WSR to predict the onset of instability in a model combustor[9]. This entire field has been recently reviewed by Huang and Yang[3].

Similar parallel efforts with the WSR can be found in chemical engineering fields. For example, Mahmoud and Fahim[8] and Ogawa et. al.[10] both use linearized WSR models to design and characterize control systems given a particular reactor and reactants. Additionally, Engell and Klatt develop controls for the non-minimum phase behaviors that can be exhibited by the linearized WSR[2].

A number of researchers have also investigated the non-linear characteristics of the WSR. Works by Park and Vlachos[14], Lignola and DiMaio[6], Olsen and Vlachos[11], and Olsen and Epstein[12, 13] detail a wide variety of nonlinear characteristics exhibited by various encarnations of the WSR. These include saddle-node bifurcation behaviors observed in constant-pressure combustion[14], cataloging the existence of stable and unstable orbits in phase space[11], analysis of static[12] and unsteady[13] characteristics, and an investigation of the reactor's initial condition response and its dependence on the model's assumptions[6].

In all cases, great value is placed on modeling the static and the linear reactor behaviors. Olsen and Vlachos[11] exemplified how the reactor's linear behavior local to equilibria offers the first insights into the nearby orbits in phase space[19]. Similarly, the most accurate predictions available regarding thermo-acoustic stability are based on linear stability. This in mind, in this work we discuss general linear characteristics of the WSR and their implications.

1.2 Formulation

WSRs have two basic assumptions that have classically been inherent to their formulation;

1. Turbulent mixing in the reactor is so strong that spatial gradients may be ignored,
2. The volume of the reactor is a constant.

These assumptions have been mapped[1, 16] into dimensionless static operating conditions to demonstrate that the WSR is appropriate when the turbulent Damköhler number,

$$Da_t = \frac{\tau_t}{\tau_c} \tag{1}$$

is much smaller than 1. Here, τ_c is the chemical time scale, and τ_t is the turbulent time scale, defined by the flame length scale in ratio with the turbulent velocity, $\tau_t = L/u'$. We shall refer back to this to help place limits on the domain over which WSR solutions are valid.

The energy equation Neglecting significant variations in pressure, the energy equation can be written as

$$c_p \dot{T} + \tau_r^{-1} \sum_i Y_{i,inlet} \left(h_i - h_{i,inlet}\right) = -\sum_j h_j \zeta_j, \tag{2}$$

where ζ_j is the rate of formation of species j in mass per unit time per unit mass of fluid. Exactly how ζ_i is calculated depends on the chemical kinetic mechanism. The three terms describe how thermal energy is accumulated, convected, and generated from reaction. The coefficient appearing in front of the convective term, τ_r, is the residence time in the reactor, given by $V\rho/\dot{m}_0$.

The heat release rate can be derived from the source term on the RHS of Equation 2, which represents the heat release per unit mass of fluid in the reactor. Multiplying by the mass in the reactor yields

$$Q = -\rho V \sum_i h_i \zeta_i. \tag{3}$$

The species equation The conservation of species can be similarly formulated

$$\dot{Y}_i + \tau_r^{-1} \left(Y_i - Y_{i,inlet}\right) = \zeta_i, \tag{4}$$

where Y_i is the mass fraction of species i, and ζ_i is its rate of formation. Similarly to the energy equation, the three terms that appear represent the specie's accumulation, convection, and generation due to reaction.

General chemical kinetics In general, a chemical mechanism is given as a series of reactions appearing in the form

$$\begin{aligned}
&(1) \quad \nu'_{A,1}A + \nu'_{B,1}B + \ldots \rightarrow \nu''_{A,1}A + \nu''_{B,1}B + \ldots \\
&(2) \quad \nu'_{A,2}A + \nu'_{B,2}B + \ldots \rightarrow \nu''_{A,2}A + \nu''_{B,2}B + \ldots \\
&\quad \vdots
\end{aligned}$$

so that $\nu'_{i,j}$ and $\nu''_{i,j}$ represent the coefficient of species i on the LHS and RHS (respectively) of reaction step j. Chemical kinetic mechanisms typically define some way of computing the number of reactions per unit time per unit mass of fluid for each of the reaction steps. Given these rates in a vector, q_j, ζ_i is given by

$$\zeta_i = \sum_j V_{i,j}\ q_j \tag{5}$$

when $V_{i,j} = MW_i(\nu''_{i,j} - \nu'_{i,j})$.

2. Simple Well-Stirred Reactor

The first of the reactors we consider herein assumes constant, species-independent specific heat and a single step reaction mechanism. As mentioned above, a number of researchers have considered simplified WSRs in various forms to produce dynamic heat release rate predictions in gas turbine engines.

When the reaction mechanism includes only one step, the formation and depletion of all species occurs proportionally, as determined by the coefficients, $V_{i,1}$. This allows the RHS of Equation 2 to be simplified, yielding

$$c_p\dot{T} + \tau_r^{-1}\sum_i Y_{i,inlet}\left(h_i - h_{i,0}\right) = -\Delta h_f \zeta_f \tag{6a}$$

$$\dot{Y}_i + \tau_r^{-1}\left(Y_i - Y_{i,inlet}\right) = \zeta_i. \tag{6b}$$

where the fuel heat release is given as a function of reactor temperature by

$$\Delta h_f = \sum_i \frac{V_i}{V_f}\, h_i. \tag{7}$$

Here, $V_{i,1}$ is abbreviated to V_i since there is only one reaction step.

With the application of constant and equal specific heats, the energy equation becomes

$$\dot{T} + \tau_r^{-1}\left(T - T_{inlet}\right) = -\frac{\Delta h_f}{c_p}\zeta_f \tag{8}$$

Since the species equation is independent of the fluid's thermal properties, it is unaffected.

Equations 8 and 6b are so similar with respect to the state variables that they can be reduced to a single equation on a single state variable. Consider the reaction

progress variable employed in the analysis of plug flow reactors by Poinsot and Veynante:

$$T = T_{inlet} + \Delta T \phi \tag{9}$$

$$Y_i = Y_{i,inlet} + \Delta Y_i \phi. \tag{10}$$

Here, ϕ is a scalar between 0 and 1 indicating the fractional progress from no combustion to complete exhaustion of the fuel. The ΔT and ΔY_i parameters refer to the change in temperature and mass fraction of species i respectively for "complete" combustion. They can be solved in terms of the enthalpy of reaction and the inlet fuel mass fraction by

$$\Delta T = \frac{\Delta h_f}{c_p} Y_{f,inlet}$$

$$\Delta Y_i = -\frac{V_i}{V_f} Y_{f,inlet}.$$

Thus, the fuel mass fraction is given by $Y_f = (1-\phi)Y_{f,inlet}$. Substituting these quantities into equation 8 and 6b yields identical equations,

$$\dot{\phi} + \tau_r^{-1}\phi = R(\phi) \tag{11}$$

In Equation 11, the function, $R(\phi)$ has units s^{-1} and is derived from ζ_i by

$$\begin{aligned} R &= \frac{\zeta_i}{\Delta Y_i} \quad \left[= -\frac{\zeta_f}{Y_{f,inlet}} \right] \\ &= -\frac{\Delta h_f}{c_p \Delta T} \zeta_f. \end{aligned}$$

It is important to note that dynamic perturbations in mass flow to the reactor will manifest themselves in Equation 11 through the appearance of $\dot{m}_0$ in τ_r. It can be shown that such perturbations would appear as

$$\dot{\phi} + \tau_r^{-1}(1+\epsilon u)\phi = R(\phi), \tag{12}$$

where $\epsilon\, u$ is the fractional change in mass flow, $\dot{m}_1/\dot{m}_0$, and ϵ is a positive dimensionless scalar amplitude of the excitation. In this way, the total mass flow is $\dot{m} = \dot{m}_0 + \dot{m}_1(t)$.

Equation 12 can be further manipulated by using a non-dimensional time scale, $\hat{t} = t/\tau_r$. We can also define a non-dimensionalize reaction rate, $\hat{R} = \tau_c R$, where the chemical time, τ_c, is defined, such that $\max(\hat{R}) = 1$. Then, Equation 11 can be rewritten as

$$\phi' + (1+\epsilon u)\phi = Da \cdot \hat{R}(\phi). \tag{13}$$

Here, the prime denotes differentiation on $\hat{t}$, and Da is the convective Damköhler number,

$$Da = \frac{\tau_r}{\tau_c} = \frac{\tau_t}{\tau_c} I = Da_t I. \tag{14}$$

The convective Damköhler number differs from the turbulent Damköhler number only in its use of the bulk velocity, $\tau_r = L/U$, instead of turbulent rms velocity, $\tau_t = L/u'$. Therefore, the two can be related by the turbulence intensity, $I = u'/U$.

If the reaction progress is further expanded in a Taylor series on ϵ, Equation 13 appears

$$\epsilon\phi_1' + (1+\epsilon u)(\phi_0 + \epsilon\phi_1) + \ldots = Da \cdot \hat{R}(\phi_0 + \epsilon\phi_1 + \ldots).$$

We obtain equations governing the steady and linear unsteady components of the solution by expanding and grouping like powers of ϵ.

$$\phi_0 - Da \cdot \hat{R}(\phi_0) = 0 \tag{15}$$

$$\phi_1' + \phi_1 \left[1 - Da \cdot \hat{R}'(\phi_0)\right] = -\phi_0 u \tag{16}$$

Characteristics By assuming constant and equal specific heats with a single-step reaction rate, Equations 15 and 16 demonstrate that the WSR can be simplified to a first order, single degree of freedom system described by only two parameters. The first and most straightforward is the Damköhler number. Secondly, the shape of the function, $\hat{R}$, also influences the static and especially the dynamic characteristics.

In any discussion of a WSR's characteristics, it is important to begin by noting that there are limits on values of Da for which the model is valid and for which the model even has a solution. The smallest Damköhler number for which there is a solution to Equation 15 is referred to as the blowoff point. Mathematically, blowoff can be defined as the condition at which the sensitivity of ϕ_0 relative to changes in Da is infinite or at which the solution is also an inflection point. By differentiating Equation 15 with respect to ϕ_0 a little bit of manipulation reveals that the reaction progress and Damköhler number at blowoff are the solutions to

$$\phi_{bo}\frac{\hat{R}'(\phi_{bo})}{\hat{R}(\phi_{bo})} = 1$$

$$Da_{bo} = \frac{\phi_{bo}}{\hat{R}(\phi_{bo})}.$$

We can observe by inspection that Da_{bo} will be on the order 1. In fact, Da_{bo} is close to, but slightly less than 1 for most combustion models.

The blowoff limit, $Da > Da_{bo}$, is a hard lower bound on Da. The well known work by Borghi[1] indicates an upper bound since the assumptions inherent to the WSR are only valid when $Da_t \ll 1$. Using Equation 14 to relate Da_t to Da, we conclude that the Simple WSR can only be used when

$$Da_{bo} < Da < I. \tag{17}$$

This regime only becomes substantial when $I \gg 1$, which is rare in practical combustion systems.

We may characterize the frequency response of heat release rate by deriving an analytical relation between $\dot{m}_1$ and Q_1 in the expansion of heat release rate, $Q = Q_0 + \epsilon Q_1 + \ldots$

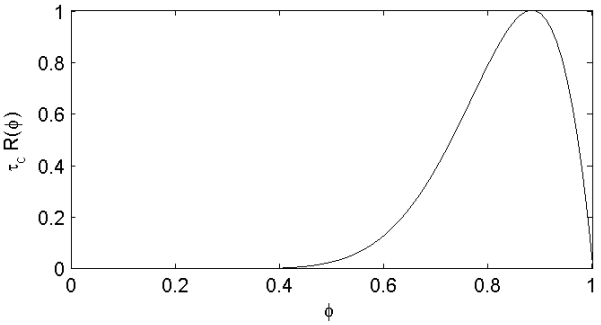

Figure 1: A typical reaction rate, $\hat{R} = \tau_c R$, as a function of ϕ

Applying a Laplace transform to Equation 16 yields the transfer function between u and ϕ_1,

$$\frac{\phi_1}{u} = \frac{-\phi_0}{\tau_r s + (1 - Da \cdot \hat{R}')}.$$

If we solve for the transfer function between mass flow and heat release, we obtain

$$\begin{aligned} \frac{Q_1}{\dot{m}_1} &= \frac{Q_1}{\dot{m}_0 u} \\ &= [c_p \Delta T \phi_0] \frac{-Da \cdot \hat{R}'}{\tau_r s + (1 - Da \cdot \hat{R}')}. \end{aligned} \tag{18}$$

Equation 18 exhibits very simple first-order dynamic characteristics shown in Table 1. Since the system is only first order, the manner in which it will couple with the surrounding acoustics is completely defined by its cutoff frequency and its DC gain. It is also immediately apparently precisely how important both Da and the shape of $\hat{R}$ are to determining the dynamic response. A typical Arrhenius expression for $\hat{R}$, which we shall use to study Equation 18, might look like the curve in Figure 1. Its precise shape is dependent on the various empirical parameters used in its definition, so that the characteristics of the WSR will also be implicitly dependent on those parameters as well.

Cutoff frequency Equation 18 has a single pole corresponding to a frequency of

$$f_c = (2\pi\tau_r)^{-1} \left[1 - Da \cdot \hat{R}'(\phi_0)\right]. \tag{19}$$

The location of the pole in the complex plane and the system's total frequency response is depicted in Figure 2.

For large Damköhler numbers, the cutoff frequency is dominated by the second term in the brackets and can therefore be estimated by $-(2\pi\tau_c)^{-1}\hat{R}'$. It is important

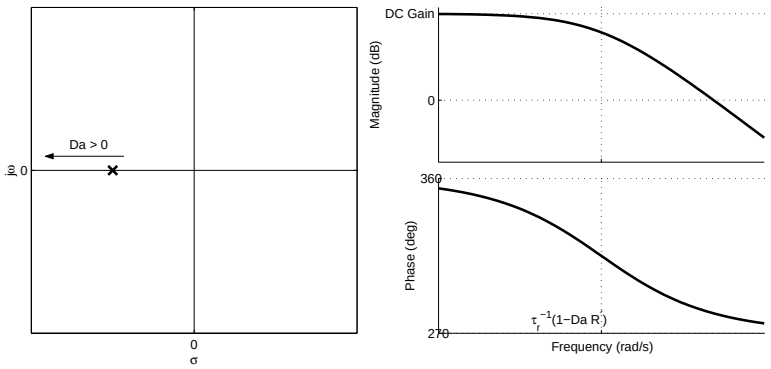

Figure 2: Simple WSR root locus and frequency response. The pole trend with respect to Damköhler number is notated on the root locus diagram with a labeled arrow.

to note that *this frequency does not correspond to the chemical time*. Though the chemical time appears as a parameter in the expression, this term can vary anywhere from 0 to 10^2 times *faster* than the chemical time scale, depending on the value of $\hat{R}'(\phi_0)$. This is the apparent "stiffness" of the flame due to the sensitivity of the reaction rate and not chemical delay. Accepting a single-step reaction mechanism precludes including any real chemical dynamics. Therefore, a Simple WSR's cutoff frequency scales with the chemical time scale for the values of Da for which the WSR is most valid.

These results can be quantified if we use a simplified Arrhenius form for the reaction rate expression,

$$\hat{R}(\phi) = A \exp\left(-\frac{T_a}{T}\right)(1-\phi)^m$$
$$T = \Delta T \phi + T_{inlet},$$

the parameter, m, defines the reaction rate's sensitivity to the extinction of fuel. Figure 3 shows the Strouhal number as a function of Da for various values of m. The dotted lines shows the same curve using the large Damköhler number estimate. This indicates the strong impact that the shape of the reaction rate function can have on the dynamics even for values of the Damköhler number on the order 10. More importantly, Figure 3 also indicates that there is no range of Da over which the Simple WSR comes even close to exhibiting cutoff frequencies at a constant value of Str.

DC gain The DC gain of the system is taken as the linear change in reaction rate per change in mass flow to the reactor.

For large Damköhler numbers, the DC gain shown in Table 1 can also be simplified. In the limit as $Da \to \infty$, the DC gain approaches $c_p \Delta T \phi_0$. The total energy

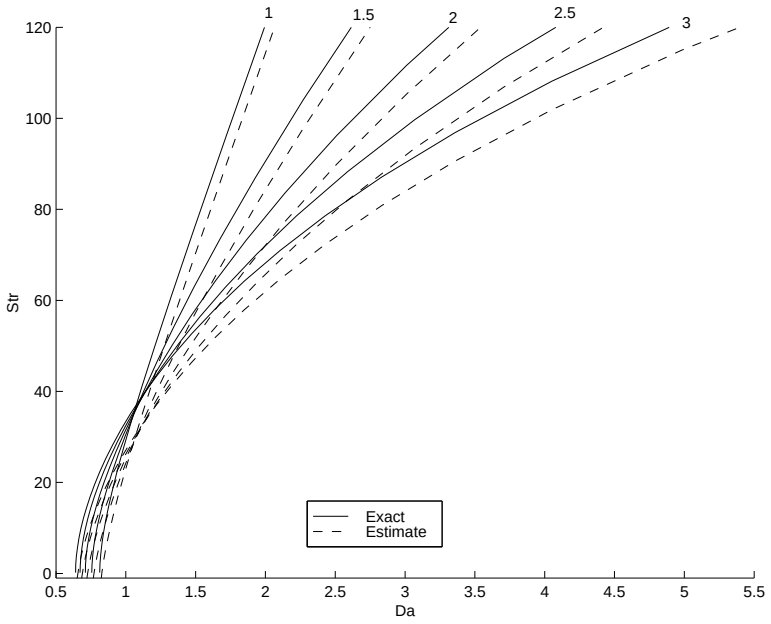

Figure 3: Strouhal number ($Str = f_c * \tau_r$) as a function of Damköhler number for various values of m.

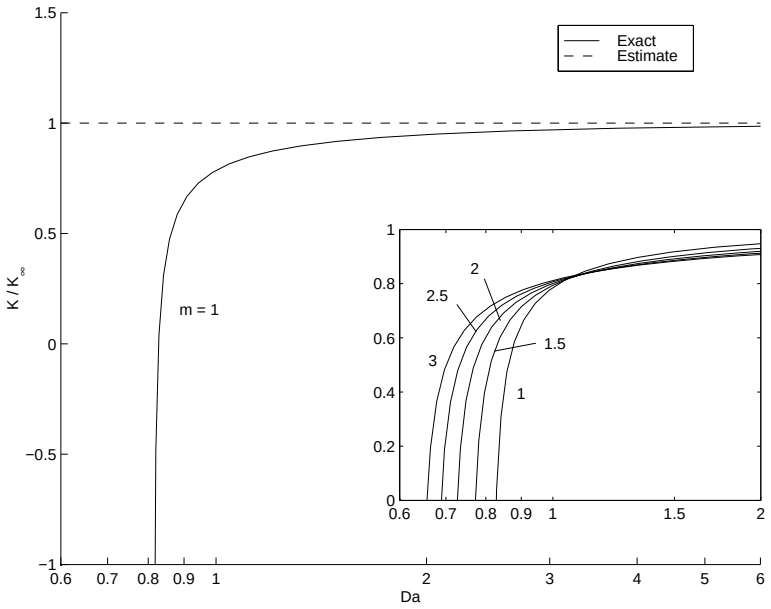

Figure 4: DC gain normalized by its asymptotic value ($\phi_0 c_p \Delta T$) and plotted with respect to Da. The embedded plot shows the gain plotted over narrow ranges of Da for various values of m.

per unit mass available from combustion of the incoming mixture is represented by $c_p \Delta T$. Since ϕ_0 indicates the fraction of fuel combusted, $c_p \Delta T \phi_0$ is the heat release per unit mass of mixture at the current operating condition. As the Damköhler number decreases, however, this intuitive estimate becomes less acurate.

Figure 4 shows the DC gain as a function of Damköhler number, normalized by the large-Da gain estimate. The embedded plot shows the minute changes in gain that occur at low Damköhler number with respect to changes in m.

Summary

- DC gain is much less sensitive to the shape of $\hat{R}$ than the cutoff frequency,
- $c_p \Delta T \phi_0$ is an excellent estimate of DC gain for $Da > O(10)$,
- Close to blowoff, $\hat{R}'$ changes sign, causing the DC gain to also change sign,
- The Simple WSR's cutoff frequency does not scale like experimental swirl-stabilized flames.

3. Non-simple Enthalpy WSR

Table 1: Dynamic characteristics of the constant-c_p, single-step kinetic WSR. Poles and zeros are reported in real units (rad/s) and the DC gain is also reported in real units (energy/mass). The right-hand column shows the estimated parameters for large Da.

	Explicit	Estimate ($Da \to \infty$)
Poles	$-{\tau_r}^{-1}\left(1 - Da \cdot \hat{R}'(\phi_0)\right)$	${\tau_c}^{-1}\hat{R}'(\phi_0)$
Zeros	∞	∞
DC Gain	$\dfrac{-Da \cdot \hat{R}'(\phi_0)}{1 - Da \cdot \hat{R}'(\phi_0)} c_p \Delta T \phi_0$	$\phi_0 c_p \Delta T$

Assuming constant and equal specific heats has long been applied because of the accompanying simplifications. The implications on the static reactor are relatively self evident, but exactly how relaxing this rigid constraint will affect the reactor's dynamics is not obvious from inspection. This will mean a migration from thinking of the enthalpy of species as parallel lines to thinking of enthalpy as a surface with dependencies on the temperature and composition of the fluid.

Since we retain the single-step reaction mechanism, Equations 6b and 6a apply, but with three very significant differences.

1. The specific heat is a function of both temperature and the fluid composition;
2. the enthalpy terms must remain empirical functions and cannot be further simplified;
3. the enthalpy of reaction, based on its definition in Equation 7, is a function of temperature.

Though all three of the above complications apply only to the energy equation, the non-simple enthalpy curves produce an asymmetry in the equations that prevent their collapse into a single equation on reaction progress. As a result, we may define a separate reaction and thermal progress variables, ϕ and ψ, such that

$$T = T_0 + \Delta T \psi$$
$$Y_i = Y_{i,0} + \Delta Y_i \phi.$$

Similar to the Simple WSR, the progress variables are allowed to vary between 0 and 1 and is assumed to be 0 at the reactor inlet. In this case, ΔY_i has exactly the same definition as in the case of the Simple WSR. Defining ΔT, however, is less trivial.

The enthalpy, which is generally given as a function of temperature and composition,

$$h(T, Y_i) = \sum_i Y_i \; h_i(T_0 + \psi \Delta T),$$

can be simplified to

$$h(\psi, \phi) = (1 - \phi) \; h_r(\psi) + \phi \; h_p(\psi),$$

where h_r and h_p are the enthalpy curves for the reactants ($\phi = 0$) and complete-combustion products ($\phi = 1$) respectively. To obtain the adiabatic temperature rise, ΔT, we enforce that the exiting enthalpy must be equal to the incoming enthalpy, so that for complete combustion,

$$h_r(0) = h_p(1),$$

where ΔT is an implicit parameter in the product enthalpy. Generally, the inversion must be performed numerically.

Nondimensionalizing as in the Simple WSR and substituting back into Equation 6a and 6b yields

$$(c_p \Delta T)\psi' + (h_r(\psi) - h_r(0)) = \Delta h(\psi) Da \cdot \hat{R}(\psi, \phi) \tag{20a}$$

$$\phi' + \phi = Da \cdot \hat{R}(\psi, \phi). \tag{20b}$$

Just as in the Simple WSR, $\hat{R} = \tau_c (Y_{f,0})^{-1} \zeta_f$. The new parameter, Δh, is given by

$$\Delta h(\psi) = h_r(\psi) - h_p(\psi).$$

It is a fortunate consequence to separating thermal and species reaction progress that the model can support not only mass flow perturbations but also perturbations in the incoming composition. Thus, when writing the perturbed equations, we let

$$\dot{m} = \dot{m}_0(1 + \epsilon u(t)) \qquad\qquad \phi_{inlet} = 0 + \epsilon v(t).$$

It is worth commenting that there are as many ways of perturbing the incoming mixture as there are species in the model, while the reaction progress approach will only support perturbations such that $Y_{i,0} = \Delta Y_i v$. Though it is an inherent limitation of reaction progress approaches that mass fractions are not allowed to vary independently, it can be shown with analysis that is tangential to the present discussion, that the relevant dynamics are still accurately represented.

The thusly perturbed reactor equations are

$$c_p \Delta T \epsilon \psi_1' + (1 + \epsilon u) \left\{ h_r(\psi_0 + \epsilon\psi_1) - h_r(0) - \left[\Delta h(\psi) - \Delta h(0) \right] \epsilon v \right\} = \Delta h(\psi_0 + \epsilon\psi_1) Da \cdot \hat{R}(\psi_0 + \epsilon\psi_1, \phi_0 + \epsilon\phi_1) + \ldots$$

$$\epsilon\phi_1' + (1 + \epsilon u)(\phi_0 + \epsilon\phi_1) - \epsilon v = Da \cdot \hat{R}(\psi_0 + \epsilon\psi_1, \phi_0 + \epsilon\phi_1) + \ldots.$$

After the necessary expansions, isolating like terms of ϵ, and several substitutions, we are left with the steady and linearized unsteady equations of motion. The steady system is given by

$$(1-\phi_0)h_r(\psi_0) + \phi_0 h_p(\psi_0) = h_r(0), \tag{21a}$$

$$\phi_0 = Da \cdot \hat{R}(\psi_0, \phi_0). \tag{21b}$$

The classic approach to solving these with minimal iteration is to assume a value for ϕ_0, invert Equation 21a to compute the corresponding value for ψ_0, and finally use Equation 21b to back-calculate the corresponding value of Da. Thus, a mapping can be made between the Damköhler number and the pair, (ψ_0, ϕ_0). Otherwise, if Da is specified directly, both equations must be solved numerically and simultaneously.

The dynamic system is given by

$$\psi_1' + \left[1 - \beta Da \cdot \hat{R}_\psi\right]\psi_1 + \left[-\beta Da \cdot \hat{R}_\phi\right]\phi_1 = -u\beta\phi_0 + (\beta - \beta_0)v, \tag{22a}$$

$$\phi_1' + \left[-Da \cdot \hat{R}_\psi\right]\psi_1 + \left[1 - Da \cdot \hat{R}_\phi\right]\phi_1 = -u\phi_0 + v, \tag{22b}$$

where β and β_0 are defined as

$$\beta(\psi_0, \phi_0) = \frac{h_r(\psi_0) - h_p(\psi_0)}{c_p(\psi_0, \phi_0)\Delta T}, \qquad \beta_0(\psi_0, \phi_0) = \frac{h_r(0) - h_p(0)}{c_p(\psi_0, \phi_0)\Delta T}. \tag{23}$$

In the case of the Simple WSR, both the static and dynamic equations collapsed conveniently on one another, but the the appearance of a thermal eccentricity, β, produces an asymmetry that prevents further simplification. The thermal eccentricity can be physically interpreted as the ratio of the adiabatic temperature rise assuming constant properties with the actual adiabatic temperature rise. As a result, β is dependent upon the values of ψ and ϕ at which the operating conditions are taken. The inlet eccentricity, β_0, appears only as a coefficient of v in the energy equation and accounts for changes in inlet enthalpy as the incoming mixture is varied.

Furthermore, if we take ψ_0 to be a function of ϕ_0 via the implicit function theorem, differentiating the energy equation with respect to ϕ_0 yields

$$\frac{\partial h}{\partial \psi}\frac{\mathrm{d}\psi_0}{\mathrm{d}\phi_0} + \frac{\partial h}{\partial \phi} = \Delta T c_p \frac{\mathrm{d}\psi_0}{\mathrm{d}\phi_0} - (h_r - h_p) = 0.$$

Therefore,

$$\frac{\mathrm{d}\psi_0}{\mathrm{d}\phi_0} = \beta. \tag{24}$$

Thus, the thermal eccentricity is an indication of how the static solution deviates from the Simple WSR as depicted in Figure 5.

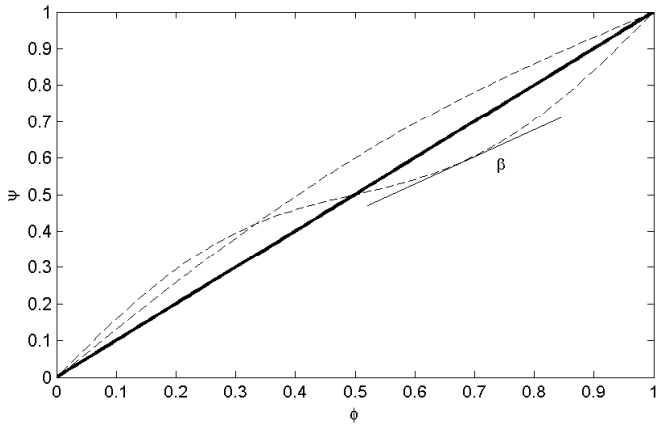

Figure 5: Example static solution paths in state space for various hypothetical enthalpy curves.

Heat release Just as with the Simple WSR, the heat release of the model is given by

$$Q = \rho\, V\, \Delta h\, {\tau_c}^{-1} \hat{R},$$

but now, in addition to considering perturbations in $\hat{R}$, there are also perturbations to Δh that cannot be neglected. The effect is quantified by the expansion of heat release, $Q = Q_0 + \epsilon Q_1 + \ldots$, where

$$Q_0 = \dot{m}_0 \Delta h Da \cdot \hat{R} \tag{25a}$$

$$Q_1 = Q_0 \left[\left(\frac{\hat{R}_\psi}{\hat{R}} + \frac{\hat{c}}{\beta} \right) \psi_1 + \frac{\hat{R}_\phi}{\hat{R}} \phi_1 \right]. \tag{25b}$$

The parameter, $\hat{c}$, is the dimensionless sensitivity of Δh to changes in ψ and is defined as

$$\hat{c} = \frac{c_{p,r}(\psi) - c_{p,p}(\psi)}{c_p(\psi, \phi)}.$$

This term has the effect of softening or stiffening the heat release rate's sensitivity to temperature by including perturbations in the temperature-dependent enthalpy of reaction.

It should also be noted that $25b$ implicitly assumes that perturbations in ρ are negligible to determining the dynamic heat release. It can be shown in a tangential analysis that density perturbations generate terms at least two orders of magnitude smaller than the predominant terms, and that their inclusion has no appreciable affect on the combustor dynamics.

State space Equations 22 are conveniently expressed in the state space form,

$$\begin{aligned} \mathbf{X}' &= \mathbf{A}\mathbf{X} + \mathbf{B}\mathbf{U} \\ Q &= \mathbf{C}\mathbf{X}, \end{aligned} \tag{26}$$

where the vectors, $\mathbf{X}$ and $\mathbf{U}$ are given by

$$\mathbf{X} = \left\{ \begin{array}{c} \psi_1 \\ \phi_1 \end{array} \right\} \qquad\qquad \mathbf{U} = \left\{ \begin{array}{c} u \\ v \end{array} \right\}$$

and the state matricies are formed from Equations 22 and 25b and are given by

$$\mathbf{B} = \left\{ \begin{array}{cc} -\beta\phi_0 & \beta - \beta_0 \\ -\phi_0 & 1 \end{array} \right\} \qquad\qquad \mathbf{C} = Q_0 \left\{ \begin{array}{cc} \frac{\hat{R}_\psi}{\hat{R}} + \frac{\hat{c}}{\beta} & \frac{\hat{R}_\phi}{\hat{R}} \end{array} \right\}$$

$$\mathbf{A} = \left\{ \begin{array}{cc} -1 + \beta Da \cdot \hat{R}_\psi & \beta Da \cdot \hat{R}_\phi \\ Da \cdot \hat{R}_\psi & -1 + Da \cdot \hat{R}_\phi \end{array} \right\}.$$

A two degree-of-freedom system will exhibit two poles and, at most, one zero. Fortunately, $\mathbf{A}$ is easily diagonalized via the linear transform, $\mathbf{X} = \mathbf{P}\mathbf{Z}$, so that

$$\mathbf{Z}' = \mathbf{P}^{-1}\mathbf{A}\mathbf{P}\mathbf{Z} + \mathbf{P}^{-1}\mathbf{B}\mathbf{U}.$$

In the process of determining an appropriate diagonalizing transform, $\mathbf{P}$, a term, $\Gamma = \hat{R}_\psi\beta + \hat{R}_\phi$, naturally appears. At this stage, its interpretation is not immediately obvious, but becomes quite significant once the transform is completed. If we select $\mathbf{P}$ such that

$$\mathbf{P} = \frac{1}{\Gamma} \left\{ \begin{array}{cc} \hat{R}_\phi & \beta \\ -\hat{R}_\psi & 1 \end{array} \right\} \qquad\qquad \mathbf{P}^{-1} = \left\{ \begin{array}{cc} 1 & -\beta \\ \hat{R}_\psi & \hat{R}_\phi \end{array} \right\},$$

the matrix, $\mathbf{P}^{-1}\mathbf{A}\mathbf{P}$, is diagonal, and the system can be divided into two decoupled differential equations,

$$z_1' = -z_1 - \beta_0 v \tag{27}$$

$$z_2' = \left(-1 + Da\Gamma\right) z_2 - \phi_0\Gamma u + \left[(\beta - \beta_0)\hat{R}_\psi + \hat{R}_\phi\right] v. \tag{28}$$

The elements of $\mathbf{Z} = \{z_1 \quad z_2\}^T$ can be computed in terms of $\mathbf{X}$ by asserting that $\mathbf{Z} = \mathbf{P}^{-1}\mathbf{X}$, resulting in

$$z_1 = \psi_1 - \beta\phi_1 \tag{29}$$

$$z_2 = \hat{R}_\psi\psi_1 + \hat{R}_\phi\phi_1. \tag{30}$$

Recalling that small changes in the static solution obey $\mathrm{d}\psi_0/\mathrm{d}\phi_0 = \beta$, changes in z_1 represent perturbations precisely normal to that curve in (ϕ, ψ) state space. Thus, if z_1 is constant, then the system is operating parallel to the static curve, and if z_1 is zero, then the system is operating *on* the static curve.

The second transformed state variable, z_2, is simply the unsteady reaction rate. These results also offer a physical interpretation for the parameter, Γ, since when $z_1 = 0$, $z_2 = \Gamma\phi_1$. Thus, Γ is the Non-simple Enthalpy equivalent of $\hat{R}'$ from the Simple WSR.

To complete the transform, the output, Q, must also be written in terms of $\mathbf{Z}$. Substitution of $\mathbf{X} = \mathbf{PZ}$ into Equation 26 yields

$$Q_1 = Q_0 \left\{ \begin{array}{cc} \frac{\hat{c}\hat{R}_\phi}{\Gamma\beta} & \left(\frac{1}{\hat{R}} + \frac{\hat{c}}{\Gamma}\right) \end{array} \right\} \mathbf{Z}. \tag{31}$$

It is also interesting to note that when Δh is constant, Equation 31 reduces to $Q_1 = Q_0\, z_2/\hat{R}$. In other words, the fractional change in heat release becomes equal to the fractional change in the reaction rate.

Frequency response to mass flow Because u does not appear in Equation 27, when the system is subject to forcing from u, $z_1 = 0$. That is certainly not because a response involving a nontrivial solution for z_1 is disallowed, but simply because, despite the asymmetry in Equations 22, the forcing with respect to u does not excite the mode that exhibits that behavior.

Redimensionalizing time and taking the Laplace transform of Equation 27, the transfer function between u and z_2 is given by

$$\frac{z_2}{u} = \frac{-\phi_0\Gamma}{\tau_r s + (1 - Da\,\Gamma)}. \tag{32}$$

Finally, substituting into Equation 31, the total transfer function is

$$\begin{aligned} \frac{Q_1}{\dot{m}_1} =& \frac{1}{\dot{m}_0}\frac{Q_1}{u} \\ =& \Delta h\phi_0 \left(1 + \hat{c}\frac{\hat{R}}{\Gamma}\right) \frac{-Da\Gamma}{\tau_r s + (1 - Da\Gamma)}. \end{aligned} \tag{33}$$

Equation 33 is almost identical to the Simple WSR except for the appearance of Γ instead of $\hat{R}'$ and the appearance of a correction factor $1 + \hat{c}\,\hat{R}/\Gamma$ to account for variations in Δh. If constant and equal specific heats are imposed, β is one and $\hat{c}$ is zero, and we recover the Simple WSR transfer function.

Because the transfer function has only a single high-frequency pole, it can be characterized by its DC gain and cutoff frequency, just as the Simple WSR. These characteristics are summarized in Table 2. The cutoff frequency bears the same behavior with respect to Da, but with an added implicit linear dependency on β through Γ.

Frequency response to mixture At first glance, the mixture perturbations have extremely different dynamic characteristics than their mass-flow counterparts. Of the two modes of excitation, mixture perturbations are the only to excite the z_1 mode, which exhibit a pole corresponding to τ_r. From the diagonal realization in

Table 2: Dynamic characteristics of the Non-simple Enthalpy, single-step kinetic WSR. Poles and zeros are reported in real units (rad/s) and the DC gain is also reported in real units (energy/mass or energy/s). The right-hand column shows the estimated parameters for large Da and small α.

	Mass	
	Exact	Estimate
Poles	$-{\tau_r}^{-1}\left(1 - Da\,\Gamma\right)$	${\tau_c}^{-1}\Gamma$
Zeros	∞	∞
DC Gain	$\Delta h \phi_0 \left(1 + \hat{c}\dfrac{\hat{R}}{\Gamma}\right) \dfrac{-Da\,\Gamma}{1 - Da\,\Gamma}$	$\Delta h \phi_0 \left(1 + \hat{c}\dfrac{\hat{R}}{\Gamma}\right)$

	Mixture	
	Exact	Estimate
Poles	$-\tau_r^{-1}$ $-{\tau_r}^{-1}\left(1 - Da\,\Gamma\right)$	$-\tau_r^{-1}$ ${\tau_c}^{-1}\Gamma$
Zeros	$-{\tau_r}^{-1}\dfrac{1 + \alpha + \hat{c}\phi_0}{1 + \alpha}$	$-{\tau_r}^{-1}(1 + \hat{c}\phi_0)$
DC Gain	$-\dot{m}_0 \Delta h \dfrac{\hat{R}_\phi}{\Gamma}(1+\alpha+\hat{c}\phi_0)\dfrac{-Da\Gamma}{1 - Da\Gamma}$	$-\dot{m}_0 \Delta h \dfrac{\hat{R}_\phi}{\Gamma}(1 + \hat{c}\phi_0)$

Table 3: Non-simple Enthalpy WSR parameters, their definitions, and their physical interpretations

Parameter	Definition	Interpretation
α	$\frac{\hat{c}\hat{R}}{\Gamma}\left(1-\frac{\beta_0}{\beta}\right)$	Quantifies the effect of varying thermal eccentricity on WSR zeros.
β	$\frac{h_r - h_p}{c_p \Delta T}$	Thermal Eccentricity: the ratio of actual adiabatic temperature rise to constant-property temperature rise.
Γ	$\hat{R}_\psi \beta + \hat{R}_\phi$	Reaction Rate Sensitivity: sensitivity of the reaction rate to low-frequency changes in ϕ.
$\hat{c}$	$\frac{c_{p,r} - c_{p,p}}{c_p}$	Specific Heat Eccentricity: dimensionless sensitivity of Δh to changes in ψ.

Equations 27 and 28, the transfer functions for the state variables with respect to v are

$$\frac{z_1}{v} = \frac{-\beta_0}{\tau_r s + 1} \tag{34}$$

$$\frac{z_2}{v} = \frac{\hat{R}_\phi}{\tau_r s + (1 - Da\,\Gamma)}. \tag{35}$$

Substituting them into 31 and performing the necessary manipulations, we arrive at the total transfer function,

$$\frac{Q_1}{v} = \dot{m}_0 \Delta h\, Da\, \hat{R}_\phi \frac{(1+\alpha)\,\tau_r s + (1 + \alpha + \hat{c}\,\phi_0)}{(\tau_r s + 1)(\tau_r s + 1 - Da\,\Gamma)}. \tag{36}$$

The parameter, α, appears as a result of the algebraic manipulations required to obtain Equation 36 and is given by

$$\alpha = \frac{\hat{c}\hat{R}}{\Gamma}\left(1 - \frac{\beta_0}{\beta}\right).$$

This expression quantifies the impact of β variations across ψ on the zero location. For most fuels, the Δh bears only a weak dependence on ψ. As such, $\beta_0 \approx \beta$ and $\alpha \approx 0$. Furthermore, the impact of this assumption is somewhat mitigated by the appearance of α both numerator terms of Equation 36. Inclusion of α is,

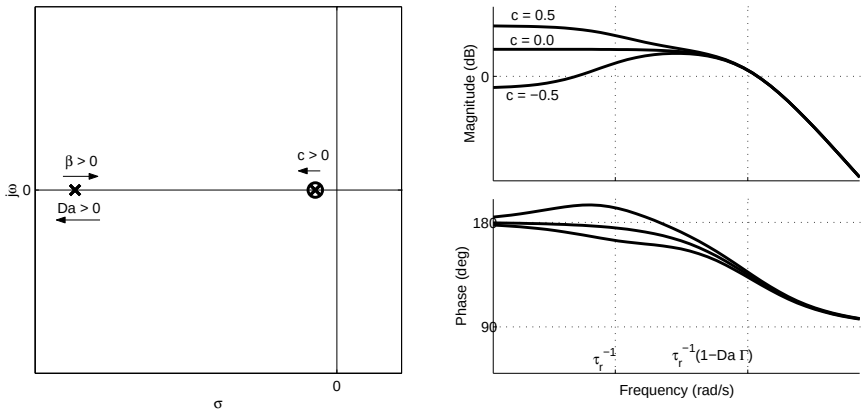

Figure 6: Non-simple enthalpy dynamic response to inlet mixture perturbations. The bode diagrams show frequency responses for several values of $\hat{c}$. The root locus plot shows pole and zero locations for $\hat{c} = 0$ with the motions notated by labeled arrows.

therefore important when $\hat{c}$ is highly nonzero or when the fuel's heat release is a strong function of ψ.

The DC gain, poles, and zeros are summarized in Table 2 and depicted in Figure 6. Because $z_1 \neq 0$, equivalence ratio perturbations exhibit a true second-order response with a single zero. The high-frequency pole that is present in both the Simple WSR and the Non-simple Enthalpy WSR is still present, but in addition to a low-frequency pole and a nearby zero.

The low-frequency pole corresponds to τ_r, regardless of other parameters. This is representative of the classic first order mixing problem that exists even in the absence of chemical reaction. Mass-flow perturbations avoid exciting such a mode altogether, but perturbations in the incoming mixture composition are unavoidably coupled with the mixing process.

The nearby zero, however, threatens to cancel the low-frequency pole. The location of the zero is an artifact of the importance of reaction rate (z_2) over any other parameter in determining the heat release rate. Since z_2 only responds with the high-frequency pole, it is only by including a Δh sensitivity to temperature through $\hat{c}$ that the zero moves from -1 and the low-frequency dynamics are revealed.

Figure 6 shows the trends in the pole and zero locations and their resulting affects on the frequency response. It should be added that the curves shown on the frequency response plot correspond to abnormally large values for $\hat{c}$. By comparison, Methane-Air reactions exhibit a $\hat{c}$ on the order -0.02. Regardless of the severity of the behavior, this indicates that the appearance of low-frequency dynamics is highly dependent on the thermal properties of the species present in the reaction.

Summary The total dynamic characteristics are summarized in Table 2 using dimensionless parameters defined in the above section and summarized in Table 3. The chief behaviors of the Non-simple Enthalpy WSR are as follows:

- The Non-simple Enthalpy WSR exhibits one high frequency and one low frequency pole with a single zero.
- Mass-flow perturbations force the zero and the low-frequency pole to cancel, leaving only the high-frequency pole.
- Perturbations in the incoming composition place the zero close to the low-frequency pole. The zero's position is dependent primarily on $\hat{c}$, so that when $\hat{c} = 0$, the zero exactly cancels the pole.
- The high frequency pole exhibits motion identical to the Simple WSR plus an added linear dependence on β.
- The low-frequency pole is always at ${\tau_r}^{-1}$.
- How severely the low-frequency dynamics affect the frequency response is indicated almost entirely by $\hat{c}$. When $\hat{c} = 0$ the low-frequency dynamics disappear.

4. Multi-step Chemical Kinetic WSR

The inclusion of multi-step chemical kinetics comes with the cost of severe complications to the approach that has thus far provided very broad parametric characterization of the WSR. Firstly, more complicated chemical kinetics introduce multiple reaction pathways and intermediate species so that the species scales, ΔY_i, are no longer well defined. Secondly, there is no longer a single convenient chemical timescale, but multiple chemical timescales so that the Damköhler number is no longer the only relevant parameter. Lastly and the most crippling of all, the system of equations is no longer conveniently analytically diagonalized without selecting a specific reaction mechanism.

Though multistep systems are more complex, there are still a number of simplifications that allow the system to serve as a broad illustration of the relevant dynamics. In a system with n species and a chemical kinetic mechanism with m reaction steps, the various reaction rate tensors and vectors have the following properties:

$$\tilde{\zeta} \in \mathbb{R}^n \qquad \tilde{q} \in \mathbb{R}^m \qquad \mathbf{V} = \{V_{i,j}\} \in \mathbb{R}^{n \times m}$$

If we impose that all species have constant and equal specific heats, then Equation 2 and 4 can be written

$$\dot{T} + {\tau_r}^{-1}(T - T_{inlet}) = -\frac{1}{c_p} \sum_i h_i \sum_j V_{i,j}\, q_j \tag{37a}$$

$$\dot{Y}_i + {\tau_r}^{-1}(Y_i - Y_{i,inlet}) = \sum_j V_{i,j}\, q_j \tag{37b}$$

From Equation, 37a, the temperature rise from each step in the mechanism naturally appears and is conveniently expressed in a vector,

$$\mathbf{H} = \left\{ \frac{\Delta h_j}{c_p} \right\} = \left\{ \frac{1}{c_p} \sum_i h_i V_{i,j} \right\}.$$

If we consider the perturbed equations — this time without non-dimensionalizing — we have that

$$\begin{aligned} \epsilon \dot{T}_1 + {\tau_r}^{-1}(1+\epsilon u)(T_0 + \epsilon T_1 - T_{inlet}) = \ldots \\ -\mathbf{H} \cdot (\mathbf{q} + \epsilon \mathbf{q}_T T_1 + \epsilon \mathbf{q}_\mathbf{Y} \cdot \mathbf{Y}_1) \\ \epsilon \dot{\mathbf{Y}}_1 + {\tau_r}^{-1}(1+\epsilon u)(\mathbf{Y}_0 + \epsilon \mathbf{Y}_1 - \mathbf{Y}_{0,inlet} - \epsilon \mathbf{Y}_{1,inlet}) = \ldots \\ \mathbf{V} \cdot (\mathbf{q} + \epsilon \mathbf{q}_T T_1 + \epsilon \mathbf{q}_\mathbf{Y} \cdot \mathbf{Y}_1). \end{aligned}$$

The steady and unsteady state variables can conveniently be grouped into state vectors,

$$\mathbf{X}_0 = \left\{ \begin{array}{c} T_0 \\ \mathbf{Y}_0 \end{array} \right\} \qquad \mathbf{X}_1 = \left\{ \begin{array}{c} T_1 \\ \mathbf{Y}_1 \end{array} \right\}.$$

Therefore, by grouping like terms of ϵ, the steady and unsteady equations are

$$\mathbf{X}_0 - \mathbf{X}_{0,inlet} = \tau_r \mathbf{A}_1 \cdot \mathbf{q} \tag{38a}$$

$$\dot{\mathbf{X}}_1 + \left({\tau_r}^{-1} \mathbf{I} - \mathbf{A}_1 \cdot \mathbf{J} \right) \cdot \mathbf{X}_1 = \mathbf{B} \cdot \mathbf{U}. \tag{38b}$$

Here, $\mathbf{A}_1$, $\mathbf{J}$, $\mathbf{B}$, and $\mathbf{U}$ are simplified expressions from the above equations, given by

$$\mathbf{A}_1 = \left\{ \begin{array}{c} -\mathbf{H}^T \\ \mathbf{V} \end{array} \right\} \qquad \mathbf{J} = \frac{\partial \mathbf{q}}{\partial \mathbf{X}} \qquad \mathbf{U} = \left\{ \begin{array}{c} u \\ \mathbf{Y}_{1,inlet} \end{array} \right\}$$

$$\mathbf{B} = \left\{ \begin{array}{cc} -\tau_r^{-1}(T_0 - T_{0,inlet}) & \mathbf{0} \\ -\tau_r^{-1}(\mathbf{Y}_0 - \mathbf{Y}_{0,inlet}) & \tau_r^{-1}\mathbf{I} \end{array} \right\}$$

Some of these vector quantities have important interpretations. The reaction rate Jacobian, $\mathbf{J}$, is the matrix transform between the unsteady state vector, $\mathbf{X}_1$, to the vector of reaction rates. The new input vector, $\mathbf{U}$, includes mass flow perturbations and inlet perturbations for any of the n species and is introduced to the system through the input matrix, $\mathbf{B}$.

The output of the system is obtained by expanding Equation 3. After the necessary substitutions, the unsteady heat release rate is

$$Q_1 = -\rho V \mathbf{H} \cdot \mathbf{J} \cdot \mathbf{X}_1. \tag{39}$$

Unfortunately, it is not at all clear how the system represented in Equations 38b and 39 behaves without selecting a specific chemical model. Since the purpose

of this analysis is to form broad, useful conclusions regarding the WSR that are independent of particular fuels or kinetic models, limiting conclusions to how the reactor behaves with respect to a specific mechanism would be unacceptably restrictive. We may note with no loss of generality, however, that if the dynamic reaction rates are given by

$$\mathbf{q}_1 = \mathbf{J} \cdot \mathbf{X}_1,$$

then Equations 38b and 39 may be rewritten as

$$\dot{\mathbf{q}}_1 = (-\tau_r^{-1}\mathbf{I} + \mathbf{J} \cdot \mathbf{A}_1) \cdot \mathbf{q}_1 + \mathbf{J} \cdot \mathbf{B} \cdot \mathbf{U} \tag{40a}$$

$$Q_1 = -\rho V \mathbf{H} \cdot \mathbf{q}_1. \tag{40b}$$

Equation 40 is obtained by multiplying Equation 38b by $\mathbf{J}$ from the left and performing the necessary substitutions. This is a state space realization with $\mathbf{q}_1$ as the state vector. This transformation hinges on being able to commute $\mathbf{J}$ in Equation 38b using the identity $\mathbf{J}\cdot\mathbf{I} = \mathbf{I}\cdot\mathbf{J}$. If we modified Equation 37a to include non-simple enthalpy effects, we would retain eccentricity coefficients in the energy equation and would be left with a diagonal matrix with unequal elements instead of the identity matrix in Equation 38b. Since the commutation of matrix multiplication is not allowed when the diagonal matrix cannot be expressed as a scalar multiple of the identity matrix, the transformation fails, and we recover the low-frequency fluid mechanical dynamics observed in the non-simple-enthalpy WSR.

General characteristics Because the matrix, $\mathbf{A}_1$, is utterly dependent on the choice of reaction mechanism, Equation 40 still represents a system that can exhibit virtually any dynamic characteristics. However, the fact that the transformation, $\mathbf{q}_1 = \mathbf{J} \cdot \mathbf{X}_1$, was successful provides a number of important implications.

A successful state space transformation cannot change the input-output relationship, nor subsequently, the transfer function. Since $\mathbf{q}_1 \in \mathbb{R}^m$ and $\mathbf{X}_1 \in \mathbb{R}^{n+1}$, and because m and n are unrelated, the transformation can change the order of the system (the number of poles). The implication is that when the system is expressed as a higher-order system, pole-zero cancellation must occur in the transfer functions so that the total dynamic behavior is preserved. Thus, the order of the system, N, is less than or equal to the smaller of m and $n+1$.

The recognition that $N \leq \min(m, n+1)$ is simply reflective of the fact that the reaction rates cannot vary with more degrees of freedom than there are state variables in the original formulation. Similarly, the species and temperature cannot vary with more degrees of freedom than there are independent reaction rates. It should also be noted that it is still possible, though not likely, that the system can be further reduced in order. This would imply that two or more of the reaction steps are linearly dependent.

The fact that the transformed state of the system can be completely represented by the reaction rates is also extremely suggestive. The transformation on the Non-simple Enthalpy WSR in Section 3 exhibited two states. The first was an eccentric state that deviated from the low-frequency operating curve while the second was

simply the unsteady reaction rate. Of these two, the former was the only to exhibit the low-frequency dynamics corresponding to the residence time. Equation 40 indicates that the Multi-step Chemical Kinetic WSR can be expressed independently of any such state variable. Subsequently the residence time dynamics that the Non-simple Enthalpy WSR exhibited will not appear in the frequency response to Equation 38b.

Typical characteristics Typically, these systems will exhibit very high-frequency poles as encountered by Park et. al.[15] and may exhibit zeros in a wide variety of configurations. The poles may be resonant (complex), but are often heavily damped enough to prevent an overshoot response.

Both pole and zero motion will occur with respect to the operating condition, but precisely how is difficult to say. One consistent behavior is that at least one pole will *always* approach the right-half plane as the operating conditions approach blowoff. This corresponds to the approach to the saddle node bifurcation that exists at the blowoff point[11].

We may exemplify these behaviors if we employ the two-step chemical kinetic mechanism proposed by Westbrook and Dryer[20] to include incomplete CO - CO_2 reaction,

$$\mathrm{C}_m\mathrm{O}_n + \left(\frac{n}{2} + \frac{m}{4}\right)\mathrm{O}_2 \rightarrow n\mathrm{CO} + \frac{m}{2}\mathrm{H}_2\mathrm{O} \tag{41a}$$

$$\mathrm{CO} + \frac{1}{2}\mathrm{O}_2 \leftrightarrow \mathrm{CO}_2. \tag{41b}$$

Reaction 41a is one-way, while reaction 41b is allowed in reverse. Therefore, the reaction rates from Westbrook and Dryer can be manipulated to the form

$$q_a = A_a \exp\left(-\frac{T_a}{T}\right) {Y_{\mathrm{C}_m\mathrm{O}_n}}^a {Y_{\mathrm{O}_2}}^b \tag{42a}$$

$$\begin{aligned} q_b =& A_{b,f} \exp\left(-\frac{T_{b,f}}{T}\right) Y_{\mathrm{CO}} {Y_{\mathrm{H}_2\mathrm{O}}}^{0.5} {Y_{\mathrm{O}_2}}^{0.25} \\ &- A_{b,r} \exp\left(-\frac{T_{b,r}}{T}\right) Y_{\mathrm{CO}_2}, \end{aligned} \tag{42b}$$

wherein the affect of density variations are neglected since reaction rate sensitivity to pressure is not needed.

Figures 7 and 8 show the response to velocity and equivalence ratio perturbations respectively of the WSR using the above mechanism. These figures show three poles and two zeros. The low-frequency poles and zeros that appear very close to the origin in both figures are exactly ${-\tau_r}^{-1}$. Because the thermal eccentricities have been eliminated, they cancel exactly (as we derived via the transformation to Equation 40).

The two remaining poles represent the dynamics of the fast and slow chemical reactions at roughly 9×10^{10}rad/s and 2.6×10^{10}rad/s respectively, and are unchanged by the mode of excitation. Only the zero moves between velocity and equivalence ratio excitations, but it is enough to change the character of the response. Just as

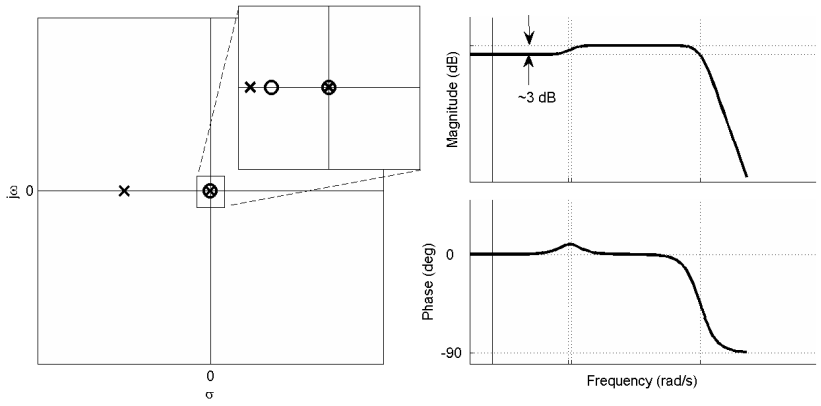

Figure 7: Multi-step chemical kinetic model response to velocity input. The stacked pole and zero that appear near the origin are at $-{\tau_r}^{-1}$, but cancel exactly.

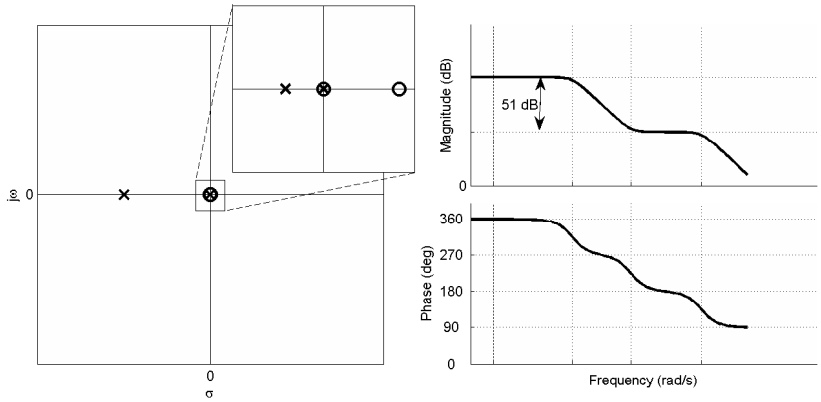

Figure 8: Multi-step chemical kinetic model response to equivalence ratio input. The zoomed-in embedded plot is not to scale.

we discussed in Section 2, there is an important distinction between the amount of time it takes for a reaction step to be completed (the chemical time scale) and how quickly that reaction rate will respond to changes in the reactor inputs (the dynamic time scale). While they are related by the fact that a faster reaction will have a faster time constant (shown in 2), they are not identical.

The results shown in Figure 8 imply that modelers attempting to use the WSR in closed-loop systems for predictions on stability must be cautious. The Nyquist and Bode criteria for assessing stability of a closed-loop system as investigated in some detail by Sattelmayer and Polifke [17], make certain assumptions regarding the nature of the system being studied. Among the most typical is that the system is minimum-phase (no zeros in the right-half plane). As Figure 8 shows, it is not at all unreasonable, however, for a flame to exhibit non-minimum phase behavior. In this event, even the corrections the authors propose to classical methods [18] might be incapable of accurately assessing stability without first knowing the number of zeros in the right-half plane. If this problem is encountered researchers should reference Engell and Klatt[2].

5. Conclusions

The linearized Well Stirred Reactor exhibits two types of separable dynamics. The first and most significant are the dynamics due to sensitivities in the chemical reaction rates. The second is the transient mixing that occurs in the reactor. For most reactor models, the governing equations can be simplified to a system of very few simple first-order equations with the Damköhler number(s) as the predominant parameter(s).

The kinetically controlled dynamics are typically high-frequency and are highly dependent on the chemical kinetic mechanism employed. At the frequencies for which most thermo-acoustic instabilities are prevalent, these dynamics are frequently sufficiently fast to be considered quasi-static except extremely close to blowoff.

The transient mixing dynamics typically only exhibit minimal impact on the frequency response if they are of any importance at all. Firstly, they only appear in the response to equivalence ratio perturbations. When they do appear, given the eccentricities of common fuels in Appendix B, they are only slight ripples in the magnitude and phase that are not likely to severely influence the stability of a closed-loop system. That these dynamics are almost completely absent in the WSR, though they are believed to be vital to swirl-stabilized combustion [7], combined with the argument that practical systems exhibit much lower Damköhler numbers solidifies the conclusion that WSR's are simply inappropriate without modification for these systems.

The appearance of right-half plane zeros in Section 4 confound most of the simplified methods for assessing stability (such as the Bode Criterion or even the Nyquist Criterion) unless the precise number of zeros can be determined a-priori. In the case of the WSR, we can accomplish exactly that, but if flames frequently exhibit this non-minimum phase behavior, then the matter must be approached with even greater care.

Remaining questions In Part II of this work, we investigate the affect of relaxing the constant-volume assumption as well as various configurations of reactor networks.

Reactor networks are interesting because by passing partially combusted mixtures into a WSR, it is allowed to operate at Damköhler numbers well below the blowoff limit, where new dynamic phenomena can occur. Moreover, they also can include infinite-order affects from recirculation.

Relaxing the constraint on volume is physically motivated since most flames are not dynamically constrained volumes. It is of great interest since it also generates entirely new dynamic phenomena and can be shown to bring new prominence to the low-frequency mixing dynamics.

Appendix A
Derivation of Governing Equations

From a more rudimentary starting point, the equations governing the accumulation of mass, species, and energy in a well mixed tank are

$$\frac{\mathrm{d}}{\mathrm{d}t}(\rho)\,V = \dot{m}_0 - \dot{m} \tag{43}$$

$$\frac{\mathrm{d}}{\mathrm{d}t}(\rho Y_i)\,V = \dot{m}_0 Y_{i,0} - \dot{m} Y_i + M\zeta_i \tag{44}$$

$$\frac{\mathrm{d}}{\mathrm{d}t}(\rho e)\,V = \dot{m}_0 e_0 - \dot{m} e + u_0 A_0 p_0 - uAp. \tag{45}$$

Here, V is the reactor volume, M is the mass in the reactor ($M = \rho V$), and e is the fluid internal energy. For this appendix only, subscripts containing 0 indicate properties at the reactor inlet, and are otherwise assumed to be the properties inside the reactor. Momentum is absent since the reactor pressure is not being modeled.

First, consider the energy equation. Recognizing that $h = e + p/\rho$, Equation 45 can be rewritten as

$$\frac{\mathrm{d}}{\mathrm{d}t}(\rho h)\,V - \dot{p}V = \dot{m}_0 h_0 - \dot{m} h. \tag{46}$$

Now, if the time derivative on the left-hand-side of Equations 44 and 46 are distributed and the density derivatives are eliminated by substituting Equation 43, we are left with

$$\dot{Y}_i M + \dot{m}_0 (Y_i - Y_{i,0}) = M\zeta_i \tag{47}$$

$$\dot{h} M + \dot{m}_0 (h - h_0) = \frac{1}{\rho}\frac{\mathrm{d}p}{\mathrm{d}t}. \tag{48}$$

Again, since the pressure in the reactor is assumed to be both steady and irrelevant to the model, the last term of the energy equation can be neglected. Since the residence time can be defined by $\tau_r = M/\dot{m}_0$, the equations simplify to

$$\dot{Y}_i + {\tau_r}^{-1} (Y_i - Y_{i,0}) = \zeta_i \tag{49}$$

$$\dot{h} + {\tau_r}^{-1} (h - h_0) = 0. \tag{50}$$

Note that the reaction rate still does not appear in the energy equation. We make it appear by writing the mixture's enthalpy in terms of its constituent species, $h = \sum_i Y_i h_i$, and substituting it to get

$$c_p \dot{T} + \sum_i \dot{Y}_i\, h_i + {\tau_r}^{-1} \left(\sum_i Y_{i,0}\, h_{i,0} - \sum_i Y_i\, h_i \right) = 0 \tag{51}$$

Finally, substituting Equation 49 to eliminate the time derivatives on Y,

$$c_p \dot{T} + {\tau_r}^{-1} \sum_i Y_{i,0} (h_i - h_{i,0}) = -\sum_i h_i \zeta_i \tag{52}$$

Appendix B
Eccentricities for various fuels

Though the values of $\hat{c}$ and β depend on the precise temperature and composition, a reasonable idea of the orders of magnitude involved may be drawn from their values under complete stoichiometric combustion at the adiabatic flame temperature. Thus, using the JANAF tables, wherein $c_p = c_p(T, \mathbf{Y})$, we may compute stoichiometric values for $\hat{c}$ and β when $\mathbf{Y}_{inlet}$ is a stoichiometric air-fuel mixture and the product mixture is given by

$$\mathbf{Y} = \mathbf{Y}_{inlet} + \mathbf{V} Y_{f,inlet}/V_f.$$

Finally, the stoichiometric, adiabatic values for $\hat{c}$ and β are given by

$$\hat{c} = \frac{c_p(T_{ad}, \mathbf{Y}_{inlet}) - c_p(T_{ad}, \mathbf{Y})}{c_p(T_{ad}, \mathbf{Y}_{inlet})} \qquad \beta = \frac{h(T_{ad}, \mathbf{Y}_{inlet}) - h(T_{ad}, \mathbf{Y})}{c_p(T_{ad}, \mathbf{Y})(T_{ad} - T_{inlet})}.$$

Table 4 shows $\hat{c}$ and β for various common gaseous fuels with an inlet temperature of 300K. The remarkable similarity between fuels is destroyed if we consider non-complete combustion or vary the inlet temperature. Methane can even be made to exhibit a negative $\hat{c}$.

In general, however, β remains relatively close to 1 and $\hat{c}$ remains quite close to 0. This is due to the fact that the reacting species only constitute a small fraction (even at stoichiometric conditions) of the fluid. As the incoming mixture becomes further and further from stoichiometric (rich or lean), the reacting species will constitute an even smaller fraction of the mixture and the eccentricities will be on an even smaller order of magnitude. The stoichiometric case is, in fact, the most eccentric case.

Table 4: Eccentricities for various fuels under stoichiometric, adiabatic combustion, with $T_{inlet} = 300K$

Fuel	Symb.	$\hat{c}$	β
Hydrogen	H_2	0.012	0.950
Methane	CH_4	0.016	0.873
Ethane	C_2H_6	0.010	0.873
Propane	C_3H_8	0.011	0.874

References

[1] R. Borghi. On the structure of turbulent premixed flames. *Recent Advances in Aeronautical Science*, pages 117–138, 1985.

[2] S Engell and K Klatt. Nonlinear control of non-minimum phase cstr. In *American Control Conference*, 1993.

[3] Ying Huang and Vigor Yang. Dynamics and stability of lean-premixed swirl-stabilized combustion. *Progress in Energy and Combustion Science*, 35:293–364, 2009.

[4] T. Lieuwen. Modeling premixed combustion - acoustic wave interactions: A review. *AIAA Journal of Propulsion and Power*, 19:765–781, 2003.

[5] T. Lieuwen and B. T. Zinn. The role of equivalence ratio oscillations in driving combustion instabilitiesin low nox turbines. In *Proceedings of the 27th International Symposium on Combustion*, pages 1809–1816, 1998a.

[6] Lignola and DiMaio. Some remarks on modeling the cstr combustion processes. *Combustion and Flame*, 80:256–263, 1990.

[7] M. Lohrmann and H. Büchner. Prediction of stability limits for lp and lpp gas turbine combustors. *Combustion Science and Technology*, 177:2243–2273, 2005.

[8] M Mahmoud and M Fahim. Closed-loop performance of inearized cstr models. In *IFAC Proceedings Series, Automation and Control in Petroleum, Petrochemical, and Desalination Industries*, pages 25–28, 1986.

[9] Christopher Martin. Systematic prediction and parametric characterization of thermo-acousticinstabilities in premixed gas tubine combustors. Master's thesis, Virginia Polytechnic Institute & State University, Blacksburg, VA, 2006.

[10] M Ogawa, H Yamamoto, T Itch, and T Katayama. Tracking controller design for a nonlinear cstr using exact linearization. In *Proceedings of the International Conference on Industrial Electrical Control and Instrumentation*, number 3, pages 2229–2234, 1991.

[11] Olsen and Vlachos. A complete p-t diagram for air oxidation of h_2 in a cstr. *Jounral of Physics: Chemistry A.*, 103:7990–7999, 1999.

[12] R Olsen and I Epstein. Bifurcation analysis of chemical reaction mechanisms i. steady state bifurcation structure. *Journal of Chemical Physics*, 94:3083–95, 1991.

[13] R Olsen and I Epstein. Bifurcation analysis of chemical reaction mechanisms ii. hopf bifurcation analysis. *Journal of Chemical Physics*, 98:2805–22, 1993.

[14] Park and Vlachos. Kinetically driven instabilities and selectivities in methane oxidation. *AICHE Journal*, 43:2083–2095, 1997.

[15] S. Park, A. Annasway, and A. Ghoniem. Heat release dynamics modeling of kinetically controlled burning. *Combustion and Flame*, 128:217–231, 2002.

[16] N. Peters. Flamelet concepts in turbulent combustion. *Proceedings of the Combustion Institute*, pages 1231–1250, 1986.

[17] T. Sattelmayer and W. Polifke. Assessment of methods for the computation of the linear stability of combustors. *Combustion Science and Technology*, 175:453–476, 2003.

[18] T. Sattelmayer and W. Polifke. A novel method for the computation of the linear stability of combustors. *Combustion Science and Technology*, 175:477–497, 2003.

[19] Steven Strogatz. *Nonlinear Dynamics And Chaos*. Westview Press, 1994.

[20] Charles Westbrook and Frederick Dryer. Simplified reaction mechanisms for the oxidation of hydrocarbon fuels in flames. *Combustion Science and Technology*, 27:31–43, 1981.